WEP Warwick Evans Publishing

International Journal of Electric Power and Energy Studies

ISSN: 3006-2004 (Print), ISSN: 3006-0826 (Online) | Volume 3, Number 2, Year 2024
DOI: https://doi.org/10.62051/ijepes.v3n2.03
Journal homepage: https://wepub.org/index.php/IJEPES/index

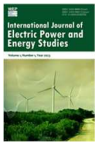

Study on Microscopic Pore Structure Characteristics of Tight Sandstone Reservoir

Xing Zhou

School of Petroleum Engineering, Xi'an Shiyou University, Xi'an 710065, China

ABSTRACT

The micro-nano scale pore throat of tight sandstone reservoir (TSR) will have a significant impact on the macroscopic seepage capacity of the reservoir. Based on X-ray diffraction (XRD), cast thin section (CTS), scanning electron microscopy (SEM), CT scanning and other testing methods, this paper studies the microscopic pore structure characteristics of tight sandstone reservoirs. The experimental results show that the quartz content of the core samples of the Chang 8 section of the tight sandstone reservoir is the highest, with an average value of 44.19%. The second is plagioclase, with an average content of 21.71%. The core samples are mainly fine-grained quartz sandstone and feldspar lithic sandstone, which are light gray as a whole, with poor oil content and basically no crude oil. The throat types are mainly flake and curved flake throats, and some tube bundle throats are developed. The maximum length of the flake throat is 348.80μm, and the width of the tube bundle throat stenosis is only 13.40μm. The total pore volume of low permeability core is $1.25\times10^{7}\mu m^{3}$, and the volume percentage is 1.19%. The volume of connected pores is $3.49\times10^{6}\mu m^{3}$, the volume percentage is 0.33%, and the proportion of connected pores is very low.

KEYWORDS

TSR; Pore Throat; Pore Throat Distribution Frequency (PTDF).

1. INTRODUCTION

The pore throat of TSR is small and narrow, the pore structure is complex, and the heterogeneity is strong [1-3]. CO_2 injection is an effective way to improve reservoir development effect. CO_2 can form miscible phase with crude oil, thereby reducing crude oil viscosity, reducing surface tension and expanding crude oil volume. In high pressure miscible displacement, the miscible system of CO_2 and crude oil is also beneficial to slow down the fingering phenomenon in the displacement process [4]. The pore throat system in tight sandstone reservoir is smaller than that of conventional sandstone, and the minimum can reach nanometer level. The micro-nano scale pore throat system is the 'bottleneck' of crude oil flowing in TSR, and its scale parameters and structural evolution mechanism in the process of CO_2 flooding are related to the development effect of the whole TSR [5]. Therefore, quantitative evaluation of the scale distribution and structural characteristics of micro-nano seepage channels in tight sandstone has important theoretical support for the efficient utilization of CO_2 flooding in tight sandstone.

2. PART OF EXPERIMENT

As shown in Fig. 1, the mineral composition was determined using a Japanese Rigaku high-resolution Smart Lab X-ray diffractometer with an output power of 3 KW, a minimum step of 0.0001°, and an incident slit of 0.05 ~ 7mm. The rock pore casting instrument developed by Chengdu Core

Technology Co., Ltd. was used for sample preparation. The high-pressure casting tank has a size of φ200×500mm, a pressure resistance of 80MPa and a temperature resistance of 200°C. The CTS test was performed using a German Leica DM2500P polarizing microscope. The light source of the device used a 12V 100W halogen lamp. The objective lens rotating disc was 5-hole position, M25 specification, and the support field of view was 25mm. The SEM test uses JSM-5500LV equipment of JEOL company to analyze the microscopic pore throat structure of rock samples. The magnification of the equipment is 5-300000 times, and the resolution is 3nm (30kv). The electron optical system can form small beam spots under large beam current, which is conducive to micro-area analysis. CT equipment is manufactured by QNSY (Tianjin) Energy Equipment Co., Ltd. Organic matter deposition test (OMDT) uses the RK-0618C petroleum asphalt four-component tester manufactured by Hebi Ruike Instrument Co., Ltd.

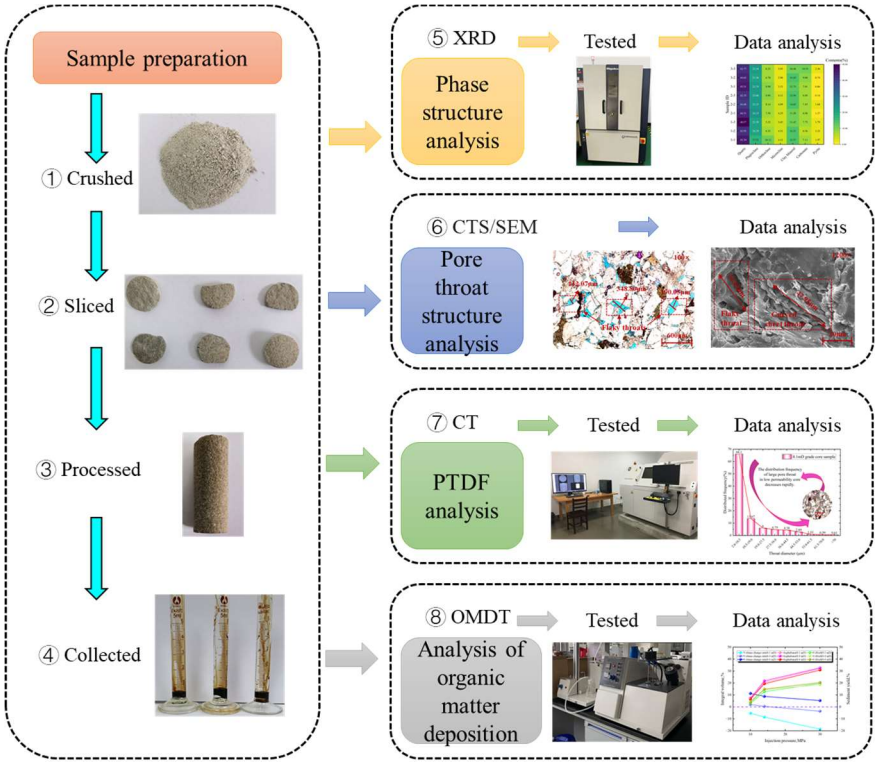

Fig. 1 Experimental process.

3. EVALUATION OF SEEPAGE CHANNEL CHARACTERISTICS

3.1. Ore Characteristics

As shown in Fig. 2, Fig. 2 (a) is the result of whole rock XRD experiment. It can be found from Fig.2 (b) that the quartz content is the highest, with an average value of 44.19%. The average content of plagioclase is 21.71%, the content of orthoclase is 8.14%, and the content of microplagioclase is 3.88%. The clay mineral content is 12.82%, and the carbonate mineral content is 7.71%. The core samples are mainly fine-grained quartz sandstone and feldspar lithic sandstone, which are light gray as a whole, with poor oil content and basically no crude oil. The contents of plagioclase, orthoclase and micro-plagioclase in the core samples are relatively high, reaching 33.72%. Feldspar minerals may produce dissolved clastic particles in CO_2 weakly acidic fluid, and migrate with the fluid to the flaky and curved flaky pore throat, resulting in a certain degree of plugging damage at the narrow pore throat of the reservoir. At the same time, carbonate minerals are also sensitive to CO_2 weak acid fluids, which will dissolve to produce metal cations such as Ca^{2+}, Mg^{2+}, and Fe^{2+} [6-7].

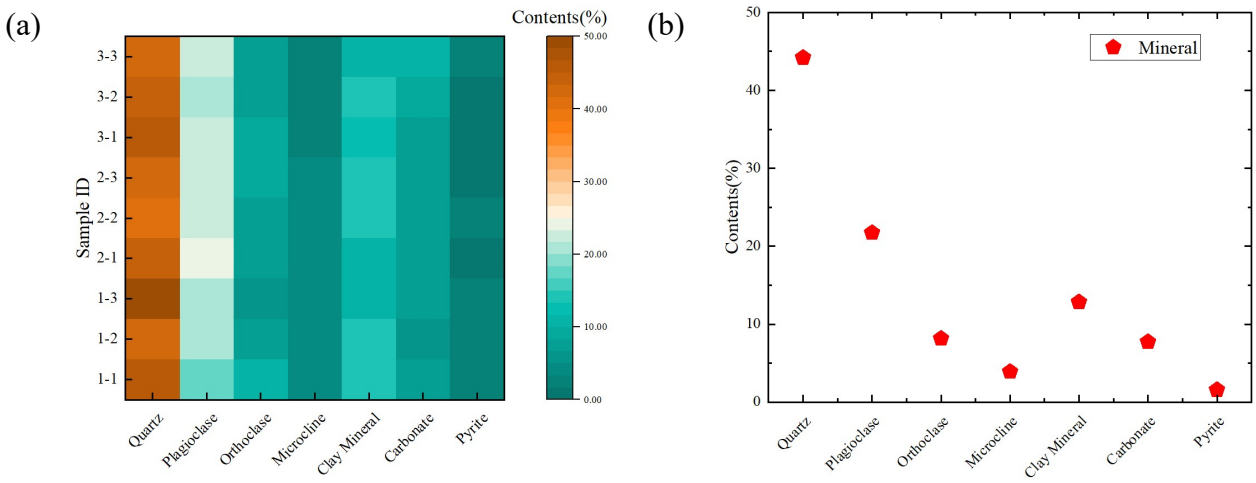

Fig. 2 The rock and mineral characteristics chart of the core samples of Chang 8 member of Yanchang Formation in Ordos Basin. (a) The whole-rock X-ray diffraction results are presented. (b) shows the average mineral content.

3.2. Types and Characteristics of Throat

As shown in fig. 3, through CTS and SEM tests, it is found that the throat types of Chang 8 section of tight sandstone reservoir are mainly sheet and curved sheet throats, and some tube bundle throats are developed. The maximum length of flaky throat is 348.80μm (Fig.3a). The narrow part of the curved sheet throat is only 14.42μm, and the narrow width of the tube bundle throat is only 13.40μm (Fig.3b). The reservoir throat size is low, the throat size is small, and the fluid is difficult to flow in it. Therefore, the permeability of tight sandstone samples is usually low. In the CO_2 flooding stage, the smaller throats are easily blocked by organic matter sediments, resulting in the damage evolution of the seepage channel and affecting the CO_2 flooding effect.

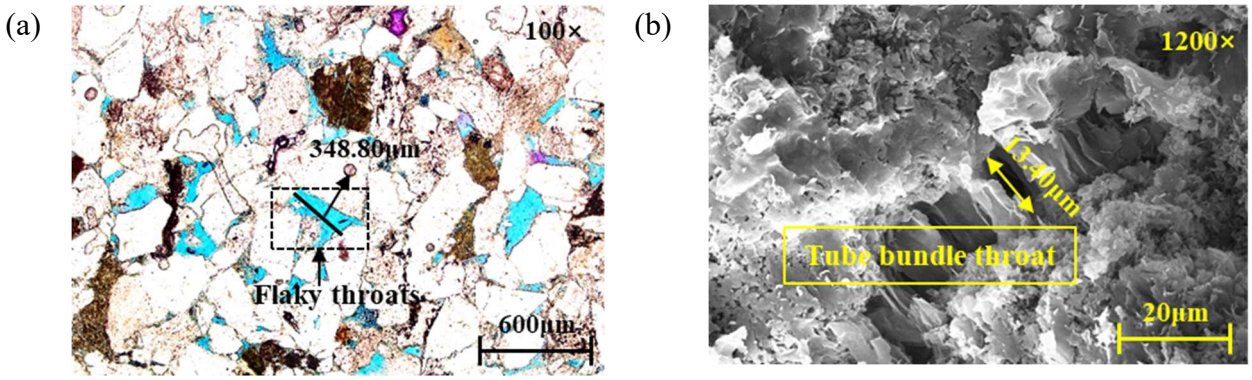

Fig. 3 The throat type and characteristics of the experimental core. (a) is the experimental result of CTS, sheet throat. (b) is the experimental result of SEM, tube bundle throat.

3.3. Analysis of Pore Throat Connectivity

As shown in fig. 4, through CT scanning, it is found that the pore throat type of Chang 8 section of tight sandstone reservoir is mainly the pore throat scale of low permeability core is small as a whole, and the distribution frequency of smaller pore throats accounts for a large proportion (Fig. 4a). As shown in Fig. 4b, the pore throat diameter of 0.1 mD core is distributed between 2.00 ~ 78.31μm, with an average of 11.11μm ; the pore throat of 2.00 ~ 10.50μm accounts for the highest proportion, reaching 66.10%, while the distribution frequency of pore throat diameter exceeding 44.5μm is only 5.10%. From the first interval to the second interval, PTDF decreased rapidly, with a decrease of

79.32%. From the third interval, PTDF remained at a low level, with an average of only 2.89%. The total pore volume of low permeability core is $1.25\times10^{7}\mu m^{3}$, and the volume percentage is 1.19%. The volume of connected pores is $3.49\times10^{6}\mu m^{3}$, the volume percentage is 0.33%, and the proportion of connected pores is very low. This makes the microscopic seepage channel of low permeability core more likely to be blocked in the CO_2 flooding stage.

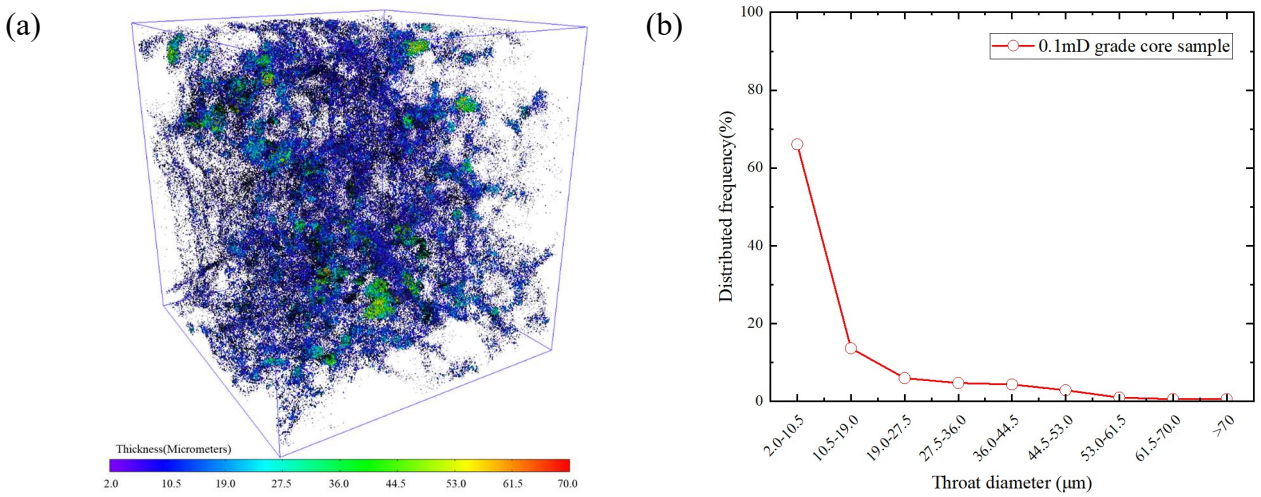

Fig. 4 The distribution characteristics of pore throats at different scales. (a) is the result of core CT scan of 0.1 mD level. (b) It is the pore throat distribution characteristics of different scales in 0.1mD core.

3.4. Evolution Characteristics of Small Seepage Channel.

As shown in fig. 5, fig. 5a is the relationship curve between the volume change rate of small seepage channel and the initial permeability. When the permeability increases from 0.1mD to 0.6mD, the volume change rate of small seepage channel increases from − 5.31% to 11.83% under 10.0MPa (immiscible) injection pressure, and the critical value P_1 is 0.335mD. The volume change rate increased from − 9.06% to 9.27% at 14.0MPa (near miscible) injection pressure, and the critical value P_2 was 0.393 mD. The volume change rate increased from − 19.04% to 5.39% at 30.0MPa (miscible) injection pressure, and the critical value P_3 was 0.463 mD. Comprehensive comparison shows that the volume change rate of small seepage channels is positively correlated with the initial permeability, that is, the higher the initial permeability, the higher the volume improvement of small seepage channels. At the same time, the greater the displacement pressure, the greater the damage to the seepage channel, the more serious the blockage, and the more obvious the phenomenon of the right shift of the zero point of the volume change rate curve.

Fig. 5 b is the relationship curve between the volume change rate of small seepage channel and the initial porosity. The porosity increases from 6.276% to 12.241%. Under the injection pressure of 10.0 MPa, the volume change rate of small seepage channel increases from − 5.31% to 2.11%, and the critical porosity value Q_1 is 9.635%. The volume change rate increased from − 9.06% to 0.56% at 14.0 MPa injection pressure, and the critical value Q_2 was 12.022%. Under the injection pressure of 30.0 MPa, the volume change rate increased from − 3.44% to 5.39%, and the critical value Q_3 was 11.358%. It is found that the volume change rate of small seepage channel is positively correlated with the initial porosity of core. The higher the effective porosity is, the lower the volume damage rate of small seepage channel is. Fig. 5 c is the relationship curve between the volume change rate of small seepage channel and injection pressure. The volume change rate of samples with permeability of 0.1mD is negative as a whole, decreasing from − 5.31% to − 19.04%. The volume change rate of the sample with permeability of 0.4mD decreased from 2.11% to − 3.44%, and the critical value of

injection pressure I_1 was 16.221 MPa. The volume change rate of the sample with a permeability of 0.6mD is positive as a whole, from 11.83% to 5.39%, and there is no zero point.

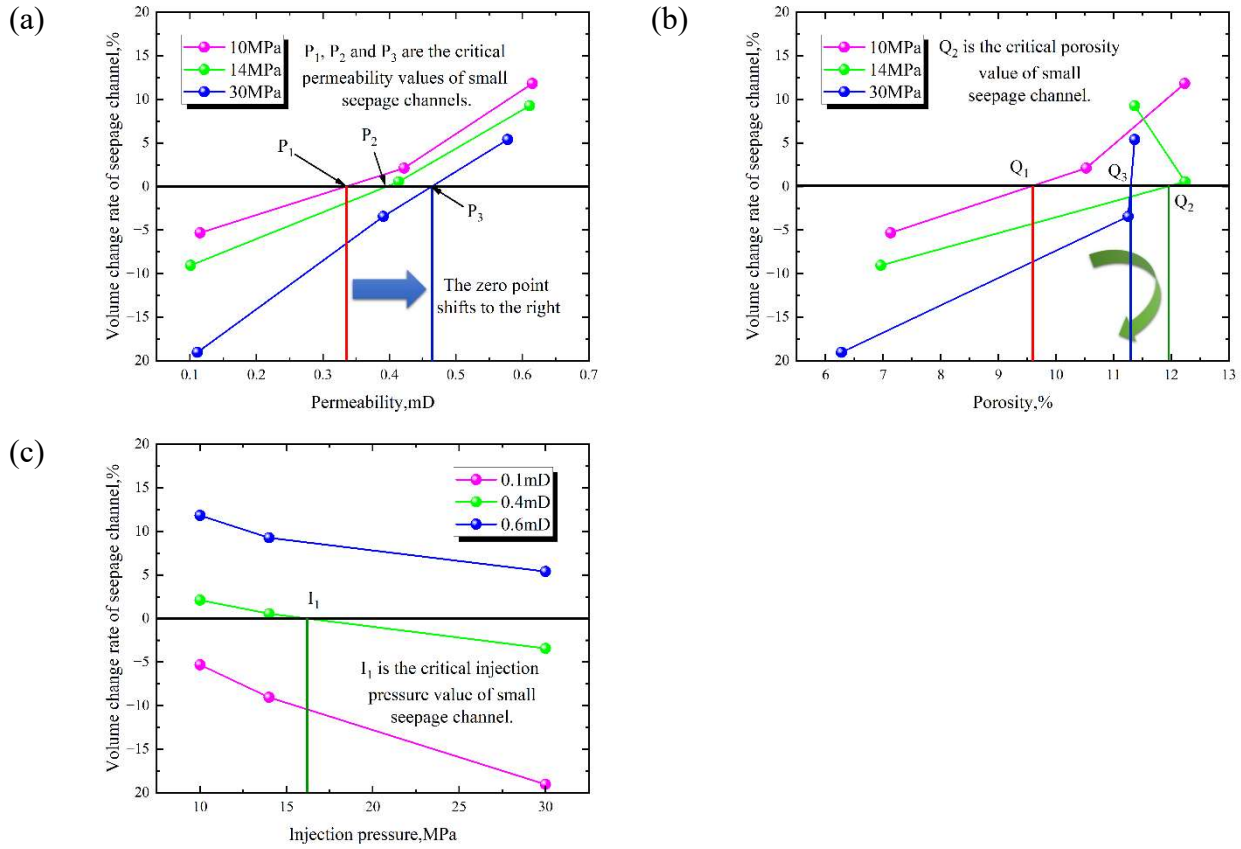

Fig. 5 Relationship between volume change rate of small seepage channel and permeability, porosity and injection pressure. (a) is the relationship between the volume change rate of small seepage channel and permeability, (b) is the relationship between the volume change rate of small seepage channel and porosity, and (c) is the relationship between the volume change rate of small seepage channel and displacement pressure.

3.5. Evolution Characteristics of Large Seepage Channel.

As shown in Fig. 6, the relationship between the volume change rate of large seepage channel and permeability (Fig. 6 a), porosity (Fig. 6 b) and injection pressure (Fig. 6 c) is shown. When the injection pressure rises from 10.0 MPa to 30.0 MPa, the critical permeability values of P_4, P_5 and P_6 are 0.359mD, 0.424mD and 0.478mD, respectively. The critical permeability value of large seepage channel increases by 0.119mD from immiscible CO_2 injection stage to miscible CO_2 injection stage, which is 0.128mD higher than that of small seepage channel, and decreases by 7.03%. It shows that the large seepage channel can resist the damage of permeability reduction caused by resin and asphaltene deposition.

At the same time, the porosity critical value Q_4 is 9.798%, Q_5 is 12.132%, Q_6 is 11.277%, and the porosity critical value has an optimal value Q_5, which is reduced by 0.915% compared with the optimal value Q_2 of small seepage channel porosity. It shows that with the increase of displacement pressure, the damage to the seepage channel increases first and then decreases, and the zero point of the volume change rate curve shifts to the right and then to the left. At the same time, it also shows that the large seepage channel has stronger ability to resist damage. Under different injection pressures, the volume change rate of the sample with a permeability of 0.1mD is negative as a whole, and the volume change rate of the sample with a permeability of 0.6mD is positive as a whole. The

difference is that the large seepage channel of the 0.4mD core crosses the zero point (I_2), and the critical value of the injection pressure of the large seepage channel is 12.884 MPa. The comprehensive analysis shows that the volume of the small seepage channel of the sample with an initial permeability of 0.4mD is improved and expanded in the immiscible flooding stage. After entering the miscible flooding, the volume of the seepage channel is blocked.

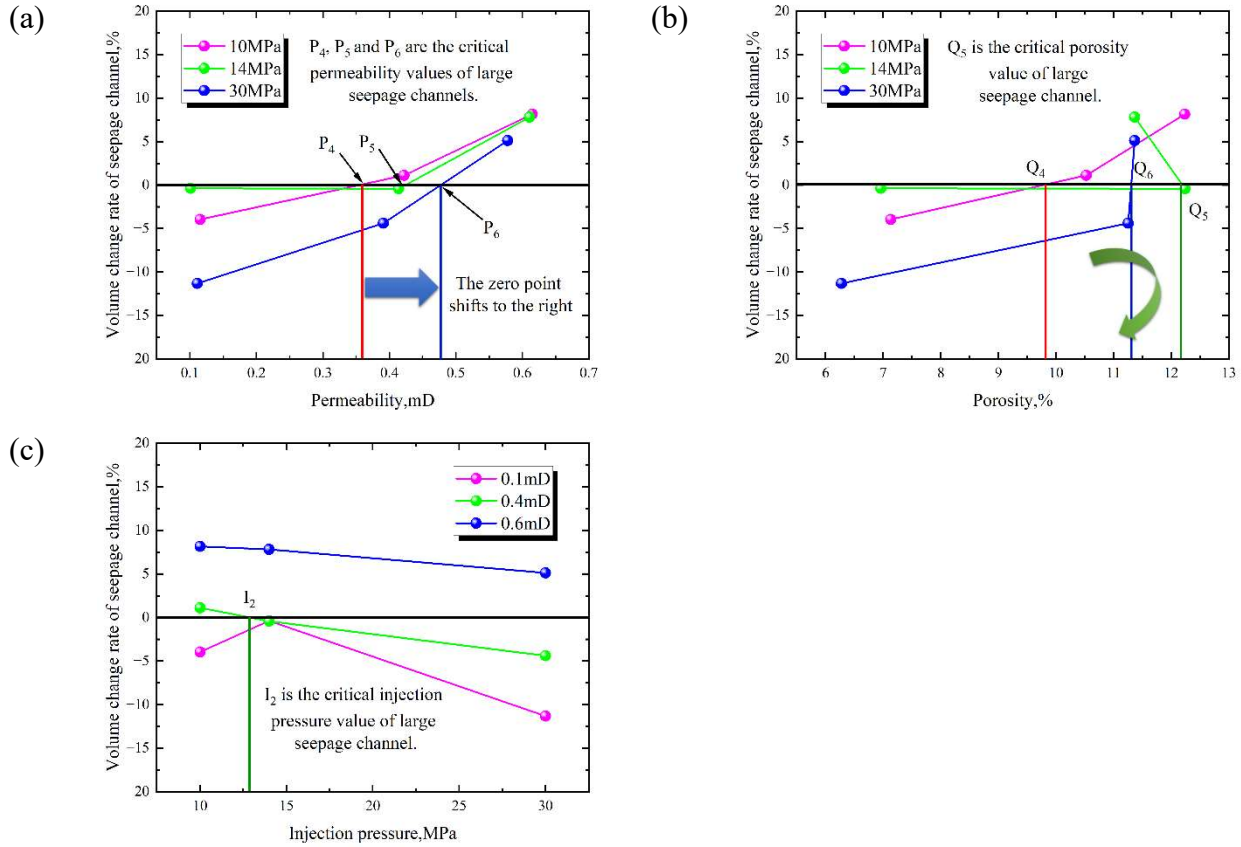

Fig. 6 The relationship between volume change rate of large seepage channel and permeability, porosity and injection pressure. (a) is the relationship between the volume change rate of large seepage channel and permeability, (b) is the relationship between the volume change rate of large seepage channel and porosity, and (c) is the relationship between the volume change rate of large seepage channel and displacement pressure.

4. SUMMARY

(1) The quartz content of core samples is the highest, with an average value of 44.19%. The second is plagioclase, with an average content of 21.71%. The core samples are mainly fine-grained quartz sandstone and feldspar lithic sandstone, which are generally light gray, with poor oil content and basically no crude oil.

(2) The throat types are mainly lamellar and curved lamellar throats, and some tube bundle throats are developed. The maximum length of lamellar throat is 348.80μm, and the width of tube bundle throat stenosis is only 13.40μm.

(3) The total pore volume of low permeability core is $1.25\times10^7\mu m^3$, and the volume percentage is 1.19%. The volume of connected pores is $3.49\times10^6\mu m^3$, the volume percentage is 0.33%, and the proportion of connected pores is very low.

ACKNOWLEDGEMENTS

Meanwhile, this research was funded by the Graduate Innovation Fund Project of Xi 'an Shiyou University (YCX2413051).

REFERENCES

[1] Liu, J.; Xie, R.; Guo, J.; Wei, H.; Fan, W.; Jin, G. Novel Method for Determining Irreducible Water Saturation in a Tight Sandstone Reservoir Based on the Nuclear Magnetic Resonance T2 Distribution. Energy Fuels 2022, 36(19), 11979-11990.

[2] Yang, Z.; Fu, J.; Guo, Q.; Lin, S.; Chen, N.; Pan, S.; Li, S. Discovery, characteristics and resource potential of continental tight oil in Triassic Yanchang Formation, Ordos Basin. China Pet. Explor. 2017, 22(06), 9-15.

[3] Ji, W.; Yu, H.; Liu, X.; Fu, H.; Yuan, B.; Yan, F.; Luo, C.; Jiang, X.; Dai, C. Oil Production Mechanism of Water Injection Huff-n-Puff for Enhancing Oil Recovery in Tight Sandstone Reservoir. Energy Fuels 2023, 37(23), 18867-18877.

[4] Zhao, S.; Fu, Q.; Ma, W. Pore-Throat Size Distribution and Classification of the Paleogene Tight Sandstone in Lishui Sag, East China Sea Shelf Basin, China. Energy Fuels 2021, 35(1), 290-305.

[5] Wu, H.; Zhang, C.; Ji, Y.; Liu, R.; Cao, S.; Chen, S.; Zhang, Y.; Wang, Y.; Du, W.; Liu, G. Pore throat size characterization of tight sandstone and its control on reservoir physical properties:a case study of Yanchang Formation , eastern Gansu , Ordos Basin. Acta Petrolei Sinica 2017, 38(08), 876-887.

[6] Pearce, J., Raza, S., Baublys, K. et al. 2022. Unconventional CO2 Storage: CO2 Mineral Trapping Predicted in Characterized Shales, Sandstones, and Coal Seam Interburden. SPE J 27: 3218–3239.

[7] Kou, Z., Wang, H., Alvarado, V. et al. 2023. Effects of Carbonic Acid-Rock Interactions on CO2/Brine Multiphase Flow Properties in the Upper Minnelusa Sandstones. SPE J 28: 754–767.